Supplementary Information

Selective C–C Bond Cleavage in Diols and Lignin Models: High-Throughput Screening of Metal Oxide-Anchored Vanadium in Mesoporous Silica

Xinnan Lu [1,2,3], Roxanne Clément [2], Yong Lu [3], Belén Albela [1], R. Tom Baker [2,*] and Laurent Bonneviot [1,*]

[1] Laboratoire de Chimie, Ecole Normale Supérieure de Lyon, Université de Lyon, 46 Allée d'Italie,
CEDEX 07,69364 Lyon, France; xinnan.lu@ku.ac.ae (X.L.); belen.albela@ens-lyon.fr (B.A.)
[2] Department of Chemistry and Biomolecular Sciences and Centre for Catalysis Research and Innovation, University of Ottawa, Ottawa, ON K1N 6N5, Canada; r.clement@uottawa.ca
[3] School of Chemistry and Molecular Engineering, East China Normal University, No. 3663 North Zhongshan Road, Shanghai 200062, China; ylu@chem.ecnu.edu.cn
* Correspondence: rbaker@uottawa.ca (R.T.B.); laurent.bonneviot@ens-lyon.fr (L.B.); Tel.: +1-613-562-5800 (ext. 7108) (R.T.B.); +33-472-72-83-91 (L.B.)

Table of Contents

Figure S1. Low-angle XRD patterns of as-made **1V-MS-L** and **1V-MS-L-cal** samples…….3
Figure S2a. Low-angle XRD patterns of **VTi-MS-T-cal**……..3
Figure S2b. Low-angle XRD patterns of **VAl-MS-L-cal**……..4
Figure S2c. Low-angle XRD patterns of **VZr-MS-L-cal** (left) and **VCe-MS-T-cal** (right).....4
Figure S3. TEM images of **1V-MS-L-cal**…….....5
Figure S4a. N_2 sorption isotherms of **MS-L-cal** and **V-MS-L-cal** at 77 K……..6
Figure S4b. N_2 sorption isotherms of **VTi-MS-T-cal** at 77 K……..6
Figure S4c. N_2 sorption isotherms of **VAl-MS-L-cal** at 77 K……..7
Figure S4d. N_2 sorption isotherms of **VZr-MS-L-cal** at 77 K…….7
Figure S4e. N_2 sorption isotherms of **VCe-MS-T-cal** at 77 K…….7
Figure S5a. ^{29}Si quantitative NMR spectrum of as-made **MS-L**……..8
Figure S5b. ^{29}Si quantitative NMR spectrum of as-made **(2.5-2.5)VAl-MS-L**……8
Figure S5c. ^{27}Al NMR spectrum of as-made **5Al-MS-L**……...9
Figure S5d. ^{27}Al NMR spectrum of as-made **(1-5)Al-MS-L**……9
Figure S6. EPR spectra of vanadium samples with Ti/Al/Zr/Ce anchors. Power = 1mW, Modulation amplitude =0.1G , T = 120 K……10
Figure S7. FT-IR spectra of as-made **V-MS-L** and **V-MS-L-cal** samples……..10
Figure S8a. UV-vis spectra of **VAl-MS-L-cal** samples……..11
Figure S8b. UV-vis spectra of **VZr-MS-L-cal** (left) and **VCe-MS-T-cal**, samples……..11

Figure S9a. Tauc plot and the corresponding edge energy of **VTi-MS-T-cal** samples based on their UV-vis spectra. E_g obtained by extrapolation of the straight line (black dots)..……12
Figure S9b. Tauc plot and the corresponding edge energy of **VZr-MS-L-cal** samples based on their UV-vis spectra……12
Figure S9c. Tauc plot and the corresponding edge energy of **VCe-MS-T-cal** samples based on their UV-vis spectra……13

Figure S10a. Effect of the nature of the Ti anchor on conversion (a) and selectivity in route a_1 (b)……13

Figure S10b. Effect of the nature of the Zr anchor on conversion (a) and selectivity in route a_1 (b)……..14

Figure S10c. Effect of the nature of the Ce anchor on conversion (a) and selectivity in route a_1 (b). ……14

Table S1. Porosity data derived from N_2 adsorption-desorption isotherms for **MS-L** and **V-MS-L-cal** samples……15

Table S2 (a). Porosity data of **VTi-MS-T-cal** derived from N_2 sorption isotherms……15
Table S2 (b). Porosity data of **VAl-MS-L-cal** derived from N_2 sorption isotherms……...16
Table S2 (c). Porosity data of **VZr-MS-L-cal** and **VCe-MS-L-cal**……16

Table S3. ^{27}Al NMR analysis of as-prepared **Al-MS-L** and **VAl-MS-L** samples……..17

Table S4. ^{29}Si quantitative NMR analysis of as-prepared samples with V and Ti/Al/Zr/Ce anchors. ……17

Table S5a. E_g from Tauc plots of Fig.S10a……..18
Table S5b. E_g from Tauc plots of Fig.S10b……18
Table S5c. E_g from Tauc plots of Fig.S10b and Fig 10d……19
Table S6a. High throughput screening of 1,2-diphenyl-2-methoxyethanol oxidation using Ti anchoring ions……...19
Table S6b. High throughput screening of 1,2-diphenyl-2-methoxyethanol oxidation using Zr and Ce anchoring ions……...20

Table S7. Oxidation of 1,2-diphenyl-2-methoxyethanol in different solvents via vanadium catalyst **(5-1)VAl-MS-L-cal**……20

Table S8. Recycling test of **(2.5-2.5)VAl-MS-L-cal** for 1,2-diphenyl-2-methoxyethanol oxidation in acetonitrile……20

REFERENCES……21

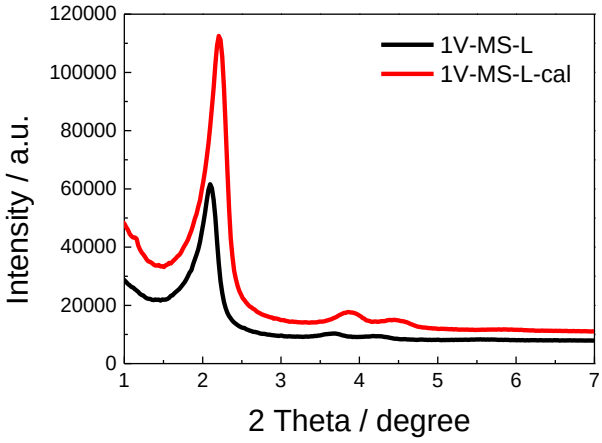

Figure S1. Low-angle XRD patterns of as-made **1V-MS-L** and **1V-MS-L-cal** samples.

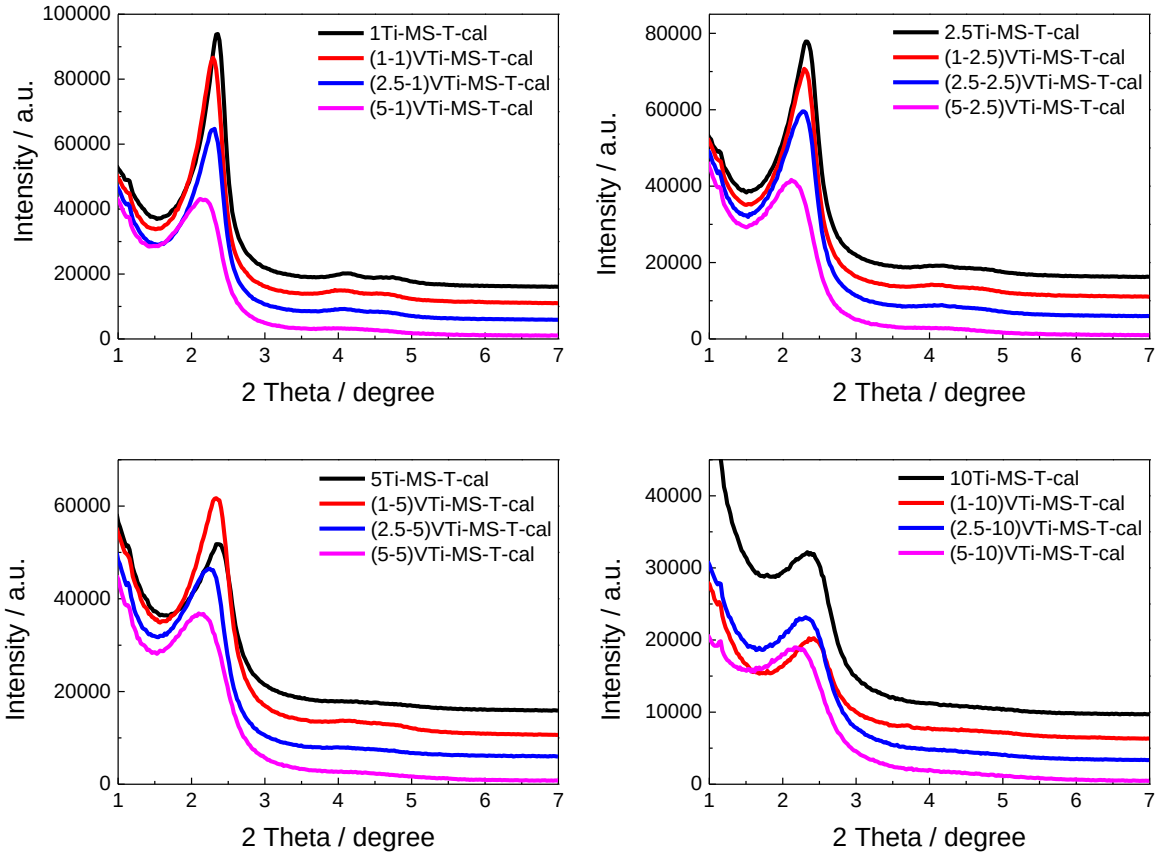

Figure S2a. Low-angle XRD patterns of **VTi-MS-T-cal**.

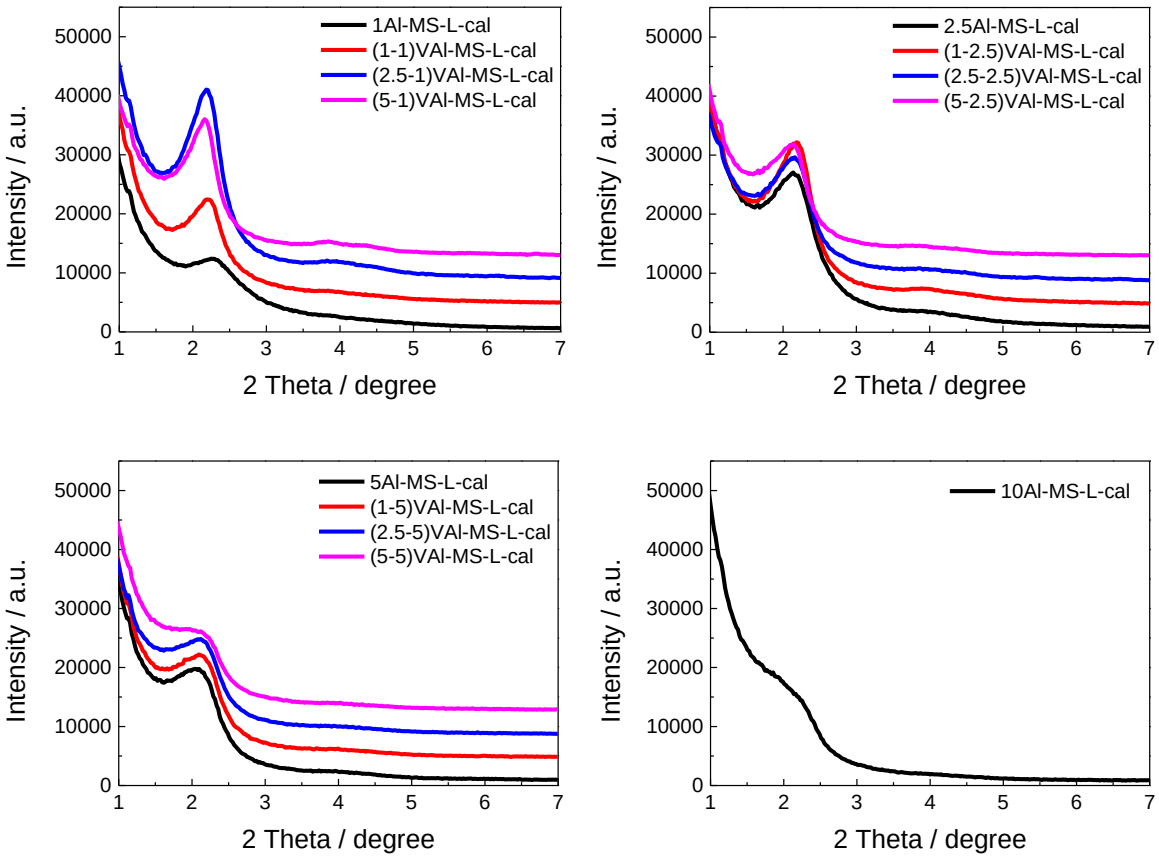

Figure S2b. Low-angle XRD patterns of **VAl-MS-L-cal**.

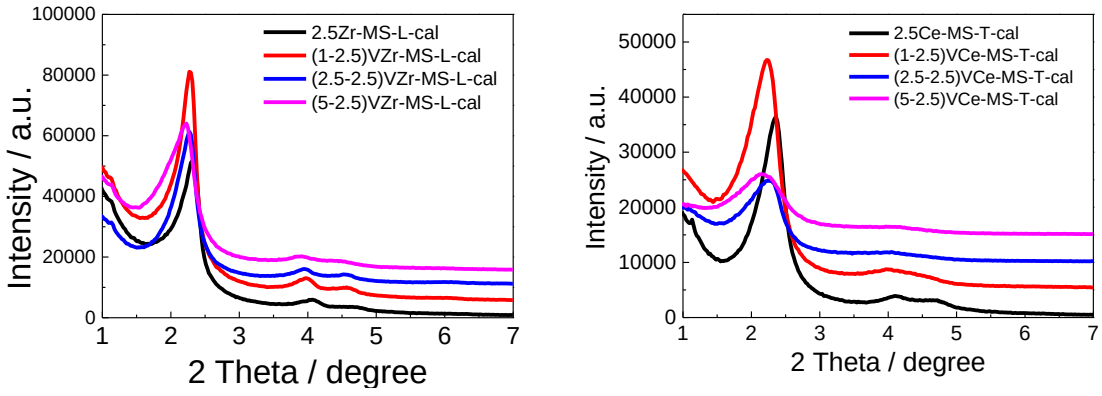

Figure S2c. Low-angle XRD patterns of **VZr-MS-L-cal** (left) and **VCe-MS-T-cal** (right).

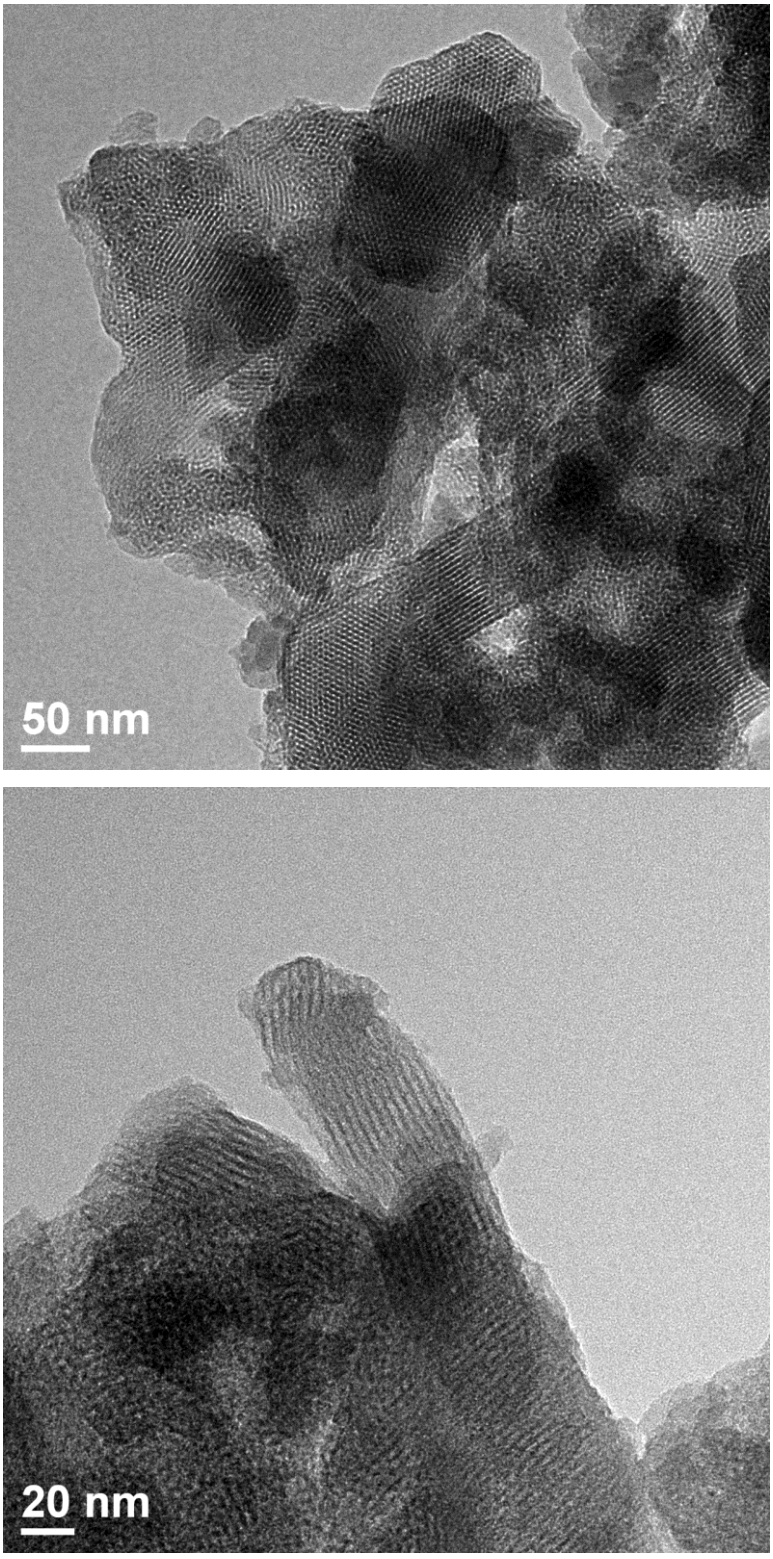

Figure S3. TEM images of **1V-MS-L-cal**. The ordered 2D hexagonal honeycomb pores can be observed clearly, the pores possessing a diameter of ca. 3 nm, and a wall thickness of about 1 nm.

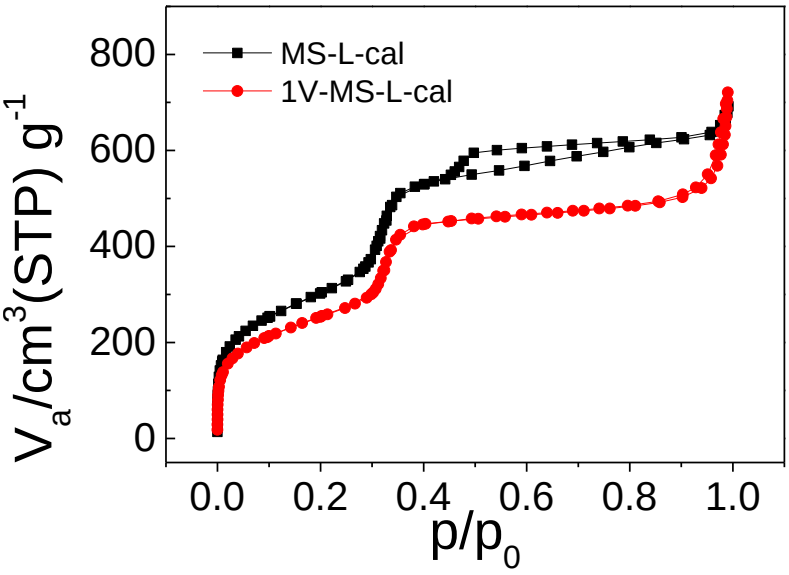

Figure S4a. N_2 sorption isotherms of **MS-L-cal** and **V-MS-L-cal** at 77 K.

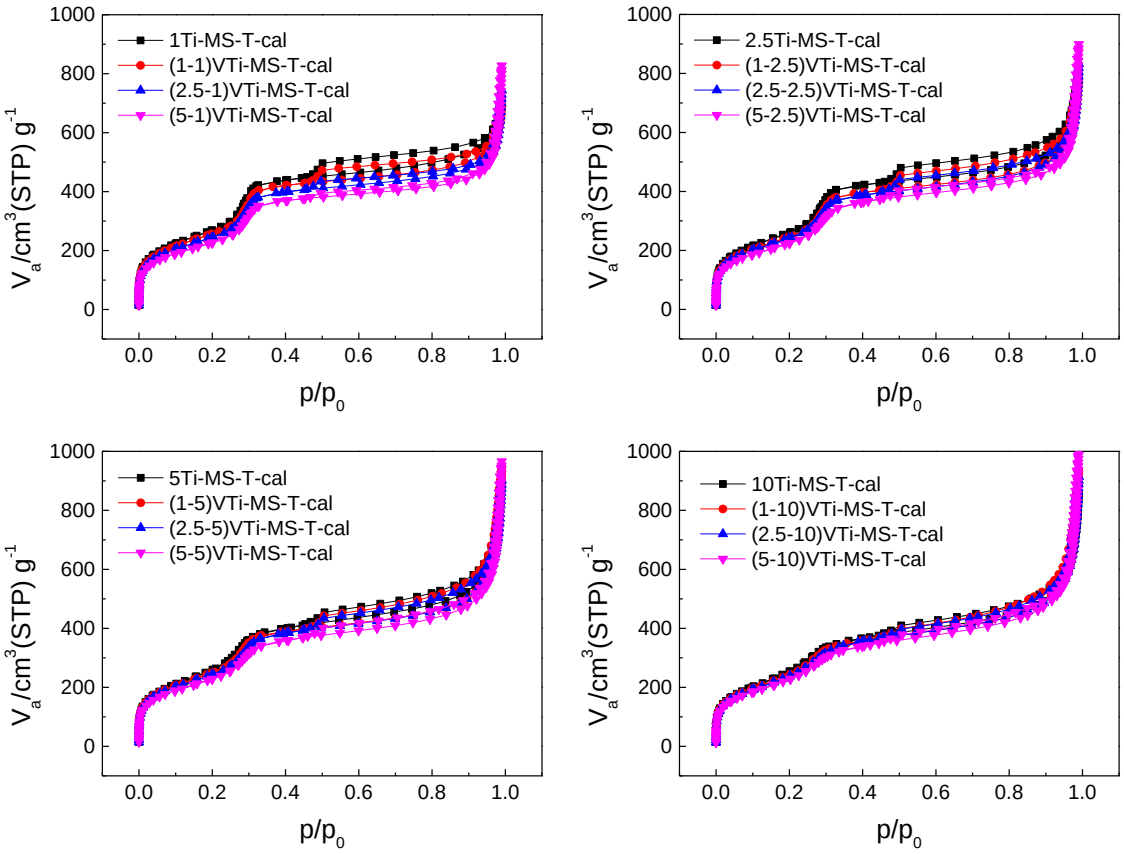

Figure S4b. N_2 sorption isotherms of **VTi-MS-T-cal** at 77 K.

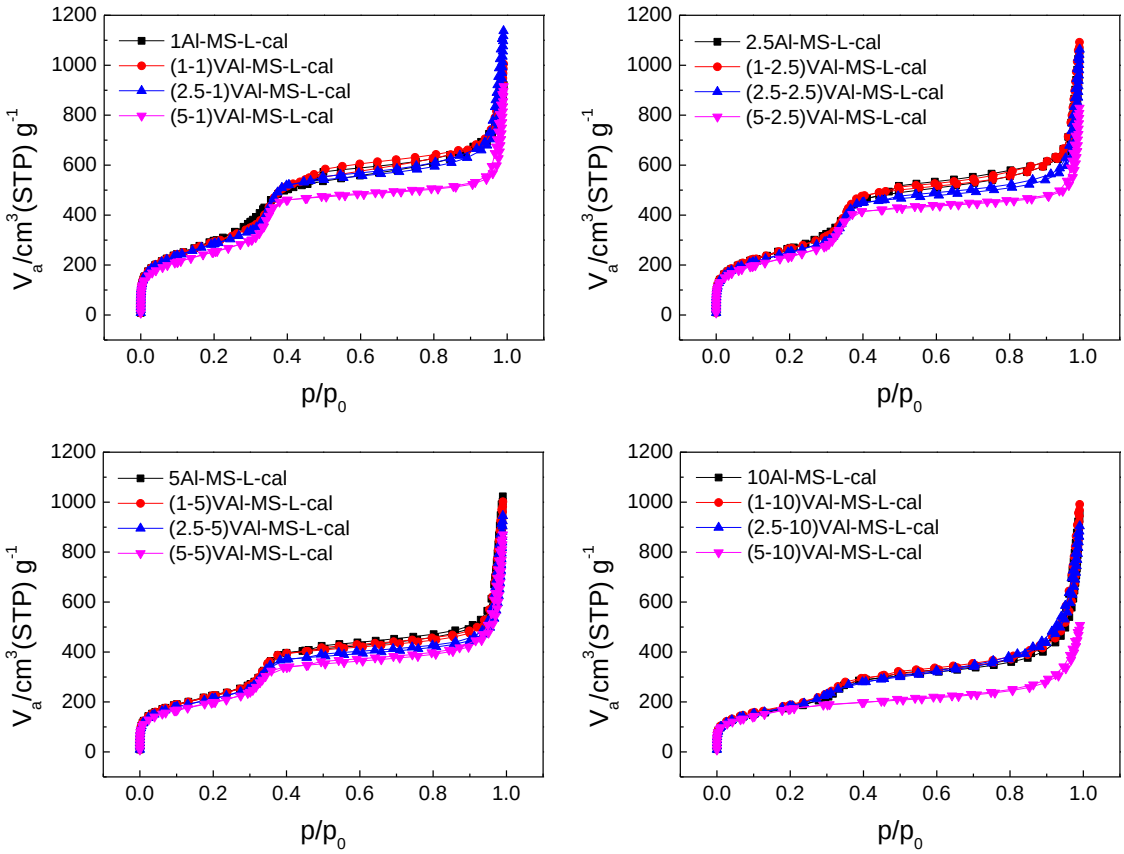

Figure S4c. N_2 sorption isotherms of **VAl-MS-L-cal** at 77 K.

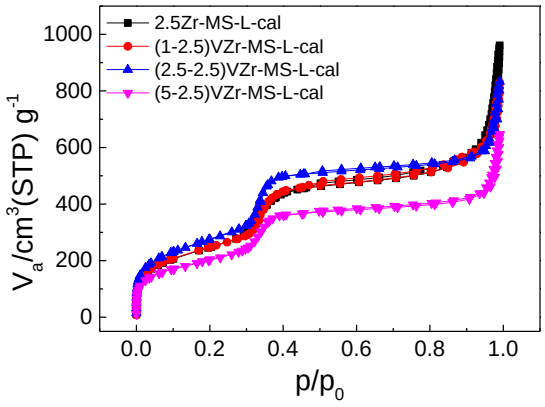

Figure S4d. N_2 sorption isotherms of **VZr-MS-L-cal** at 77 K.

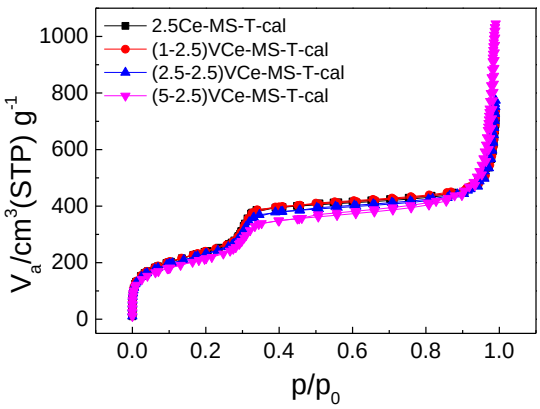

Figure S4e. N_2 sorption isotherms of **VCe-MS-T-cal** at 77 K.

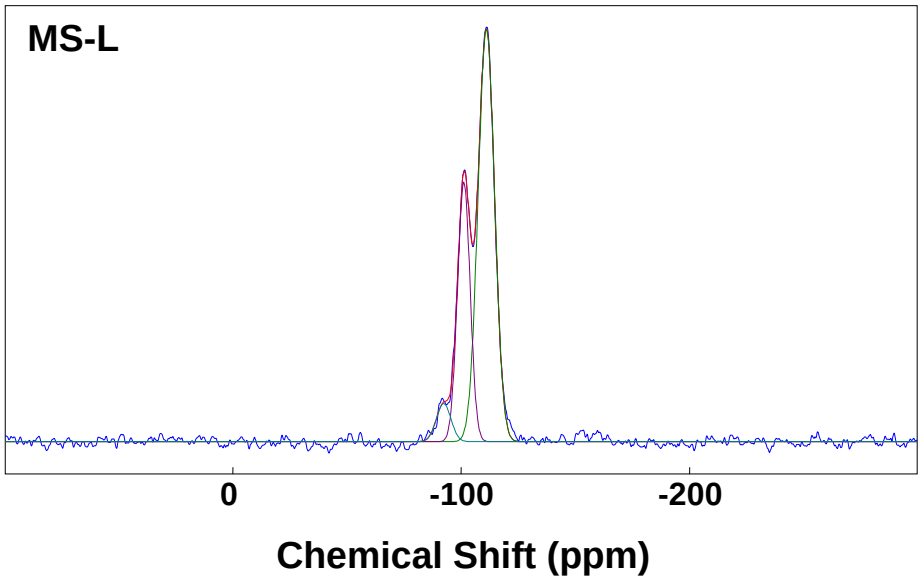

Figure S5a. ^{29}Si quantitative NMR spectrum of as-made **MS-L**.

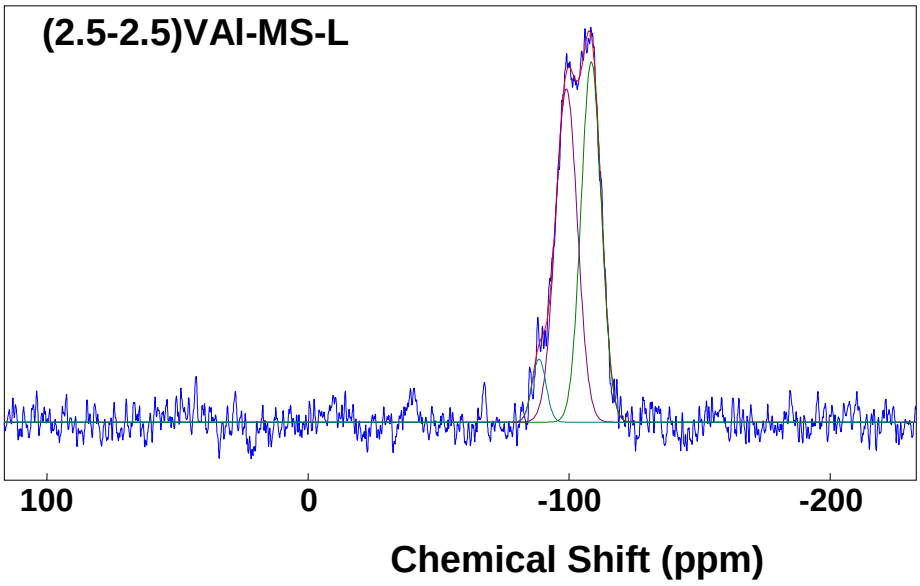

Figure S5b. ^{29}Si quantitative NMR spectrum of as-made **(2.5-2.5)VAl-MS-L**.

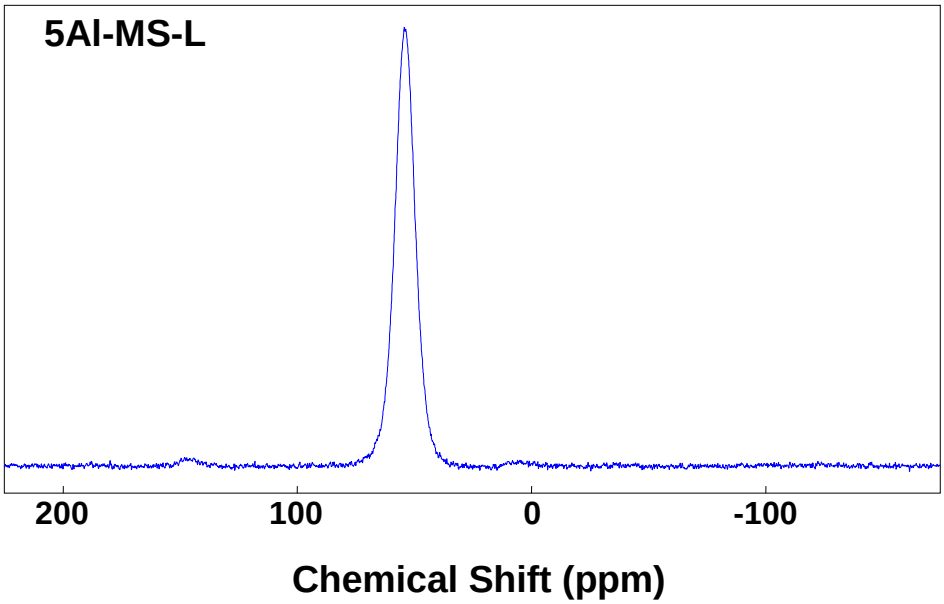

Figure S5c. ^{27}Al NMR spectrum of as-made **5Al-MS-L**.

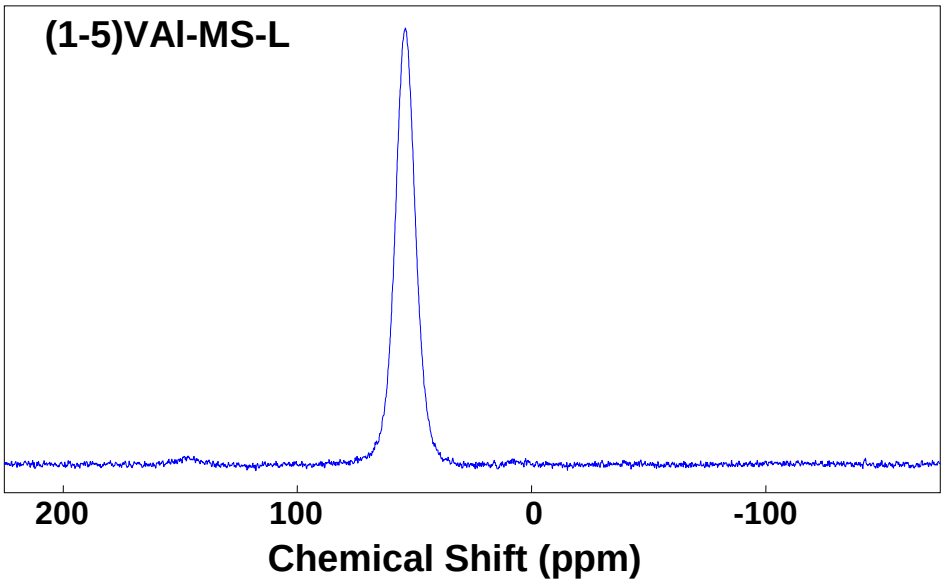

Figure S5d. ^{27}Al NMR spectrum of as-made **(1-5)Al-MS-L**.

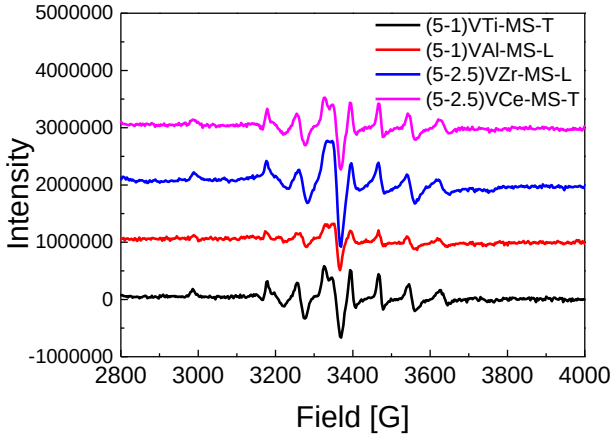

Figure S6. EPR spectra of vanadium samples with Ti/Al/Zr/Ce anchors. Power = 1mW, Modulation amplitude =0.1G , T = 120 K.

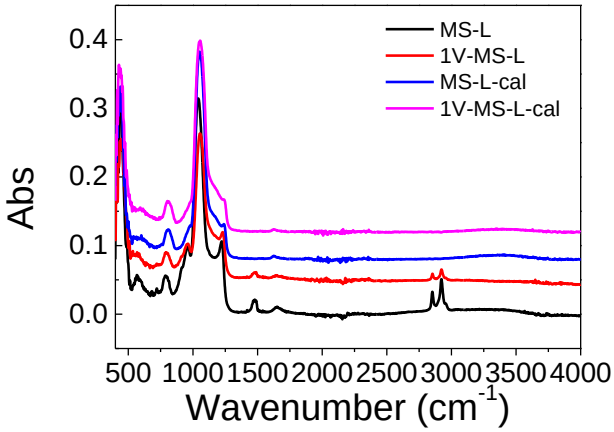

Figure S7. FT-IR spectra of as-made **V-MS-L** and **V-MS-L-cal** samples.

From the FT-IR spectra of as-made **V-MS-L** (**Figure S7**), the band at about 1490 cm^{-1} comes from the C-H bending (δ_{C-H}) vibrations of surfactant, and the bands in the region of 2800 cm^{-1} to 3000 cm^{-1} are derived from the C-H stretching (ν_{C-H}) vibrations of -CH_3- and -CH_2- in the surfactant; after calcination at 550 ^oC for 6 h, these bands disappeared, indicating total removal of organic surfactant template. The band derived from Si-OH bond stretching vibration of the silanol groups at 960 cm^{-1} decreased after calcination due to condensation of silanol groups inside the pore walls during calcination. With increasing vanadium loading, bands between 1000 and 1200 cm^{-1} were enhanced due to the stretching vibration of V=O, [1,2] which overlaps with the Si-O-Si asymmetric stretching vibration.[3] The FT-IR spectra of vanadium-incorporated MCM-41 with Ti/Al/Zr/Ce anchors are all in accordance with the bands of **V-MS-L** and **V-MS-L-cal**.

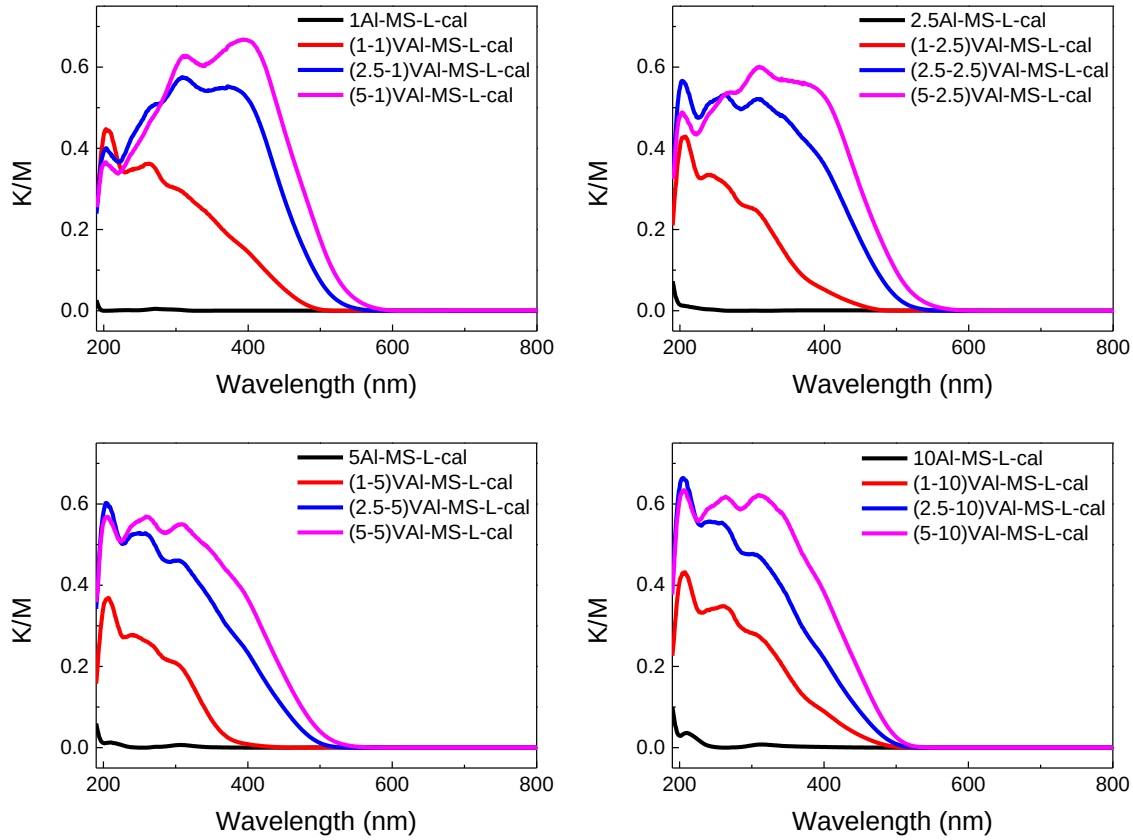

Figure S8a. UV-vis spectra of **VAl-MS-L-cal** samples.

MS-L-cal was used as blank, and before measurement, samples were diluted in **MS-L-cal** to keep the spectral intensity in the range of 0.2-0.8 Kubelka-Munk (K/M).

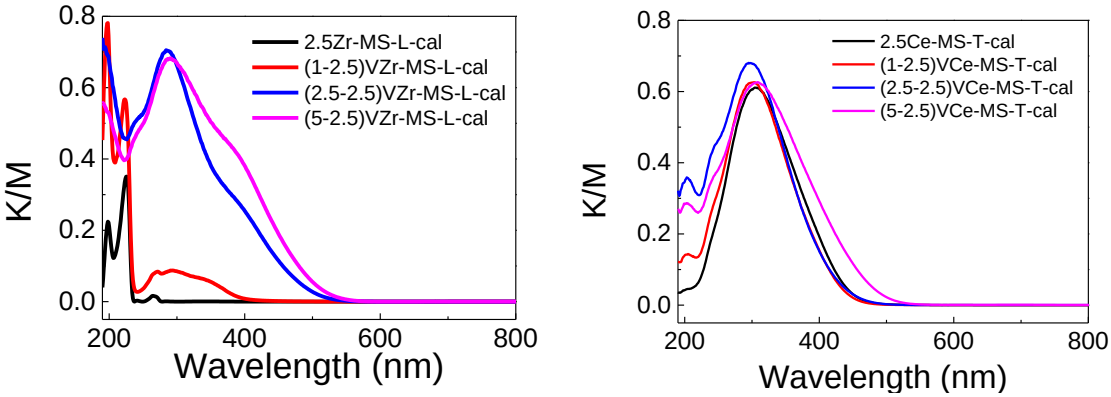

Figure S8b. UV-vis spectra of **VZr-MS-L-cal** (left) and **VCe-MS-T-cal** (right).

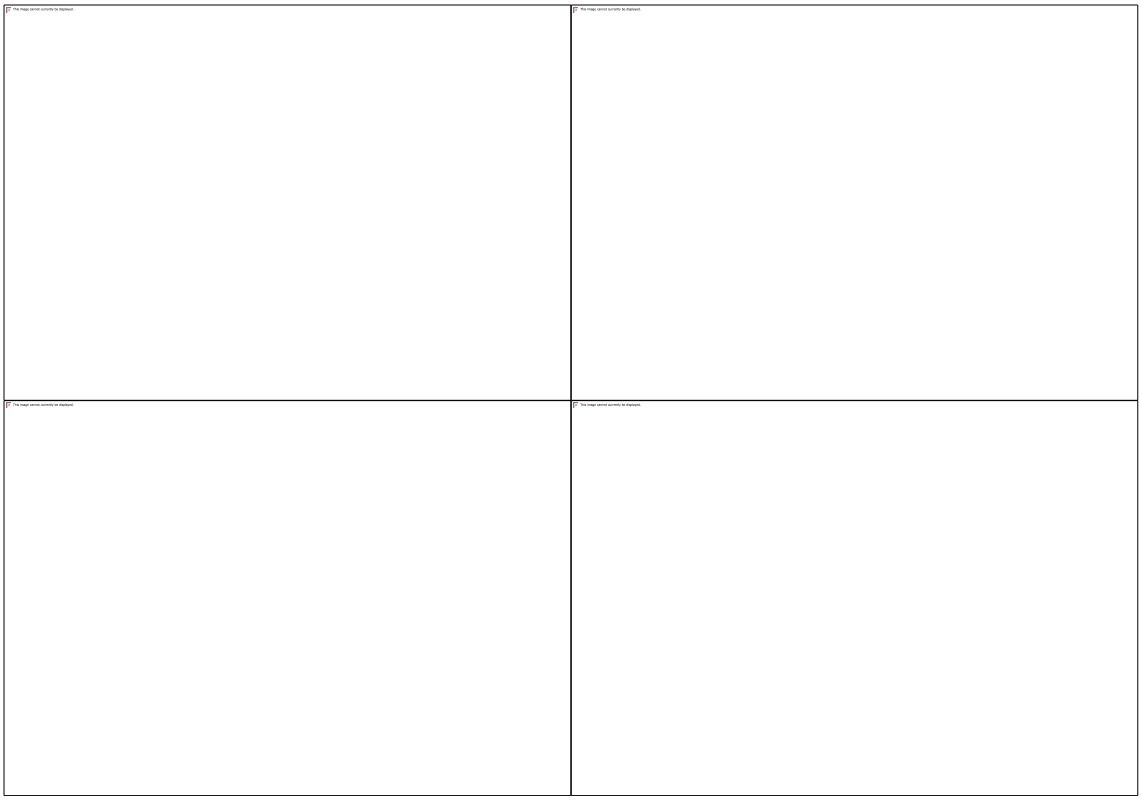

Figure S9a. Tauc plot and corresponding edge energy of **VTi-MS-T-cal** samples based on their UV-vis spectra. E_g obtained by extrapolation of the straight line (black dots).

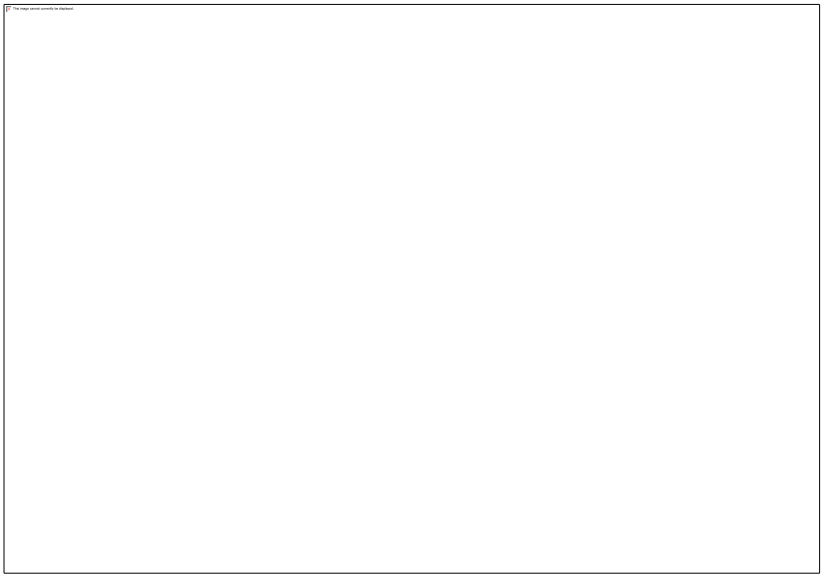

Figure S9b. Tauc plot and corresponding edge energy of **VZr-MS-L-cal** samples based on their UV-vis spectra.

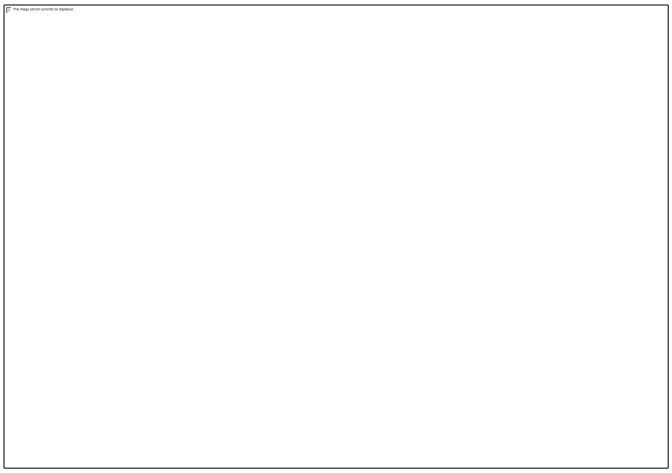

Figure S9c. Tauc plot and corresponding edge energy of **VCe-MS-T-cal** samples based on their UV-vis spectra.

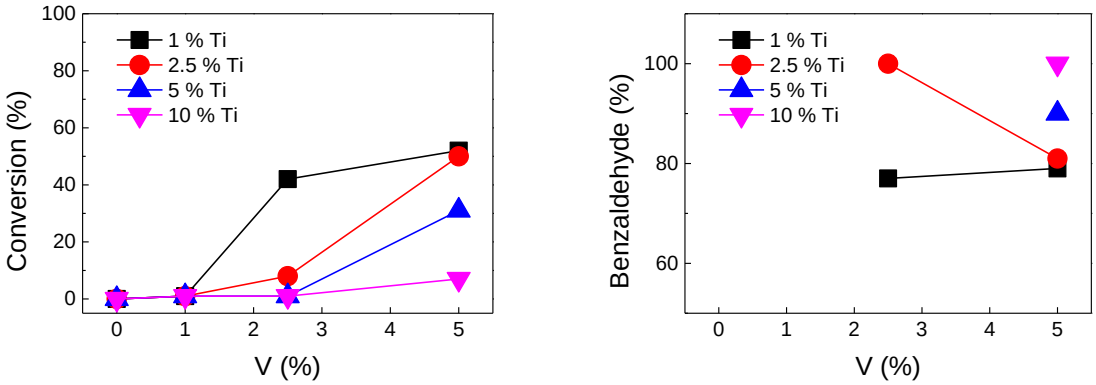

Figure S10a. Effect of the nature of the Ti anchor on conversion (a) and selectivity in route a_1 (b).

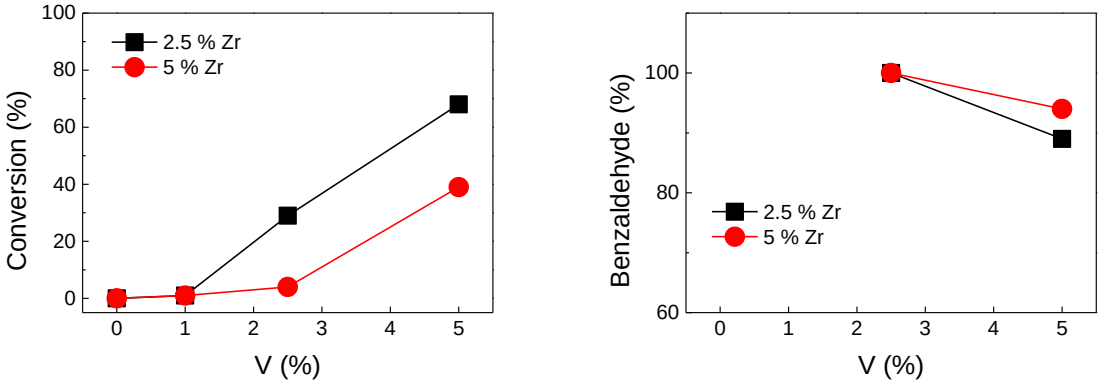

Figure S10b. Effect of the nature of the Zr anchor on conversion (a) and selectivity in route a_1 (b).

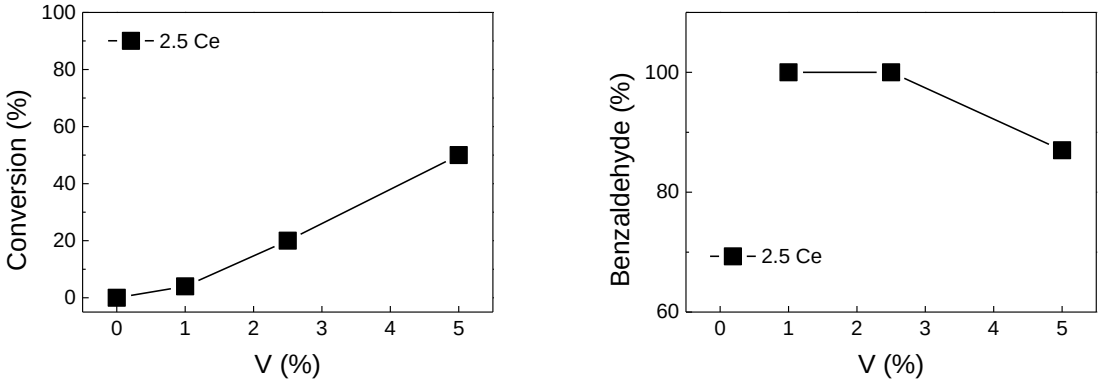

Figure S10c. Effect of the nature of the Ce anchor on conversion (a) and selectivity in route a_1 (b).

Table S1. Porosity data derived from N_2 adsorption-desorption isotherms for **MS-L** and **V-MS-L-cal** samples.

Sample	a_0[a] (nm)	V_{total}[b] ($cm^3\ g^{-1}$)	V_p[c] ($cm^3\ g^{-1}$)	S_{BET}[d] ($m^2\ g^{-1}$)	d_{HK}[e] (nm)	d_{BdB}[f] (nm)	$T_{w\ BdB}$[g] (nm)	C
MS-L-cal	4.6	1.05	0.90	1107	3.0	3.5	1.1	83
1V-MS-L-cal	4.6	1.10	0.67	929	3.1	3.6	1.0	81

(a) Hexagonal lattice parameter calculated from XRD, $a_0 = 2d_{100}/1.732$, accuracy ± 0.1 nm; (b) V_{total} at $p/p_0 = 0.99$, accuracy $\pm 0.01\ cm^3g^{-1}$; (c) V_p at $P/P_0 = 0$ on the adsorption plateau of t-plot, accuracy $\pm 0.01\ cm^3g^{-1}$; (d) from BET equation at $0.05 \leq p/p_0 \leq 0.16$, accuracy $\pm 50\ m^2g^{-1}$; (e) pore diameter extrapolated from Horvath-Kawazoe method, accuracy ± 0.1 nm; (f) pore diameter extrapolated from Broekhoff and De Boer method, accuracy ± 0.1 nm; (g) pore wall thickness calculated from a_0-d_{BdB}, accuracy ± 0.2 nm.

Table S2(a). Porosity data of **VTi-MS-T-cal** derived from N_2 sorption isotherms.

Sample	a_0[a] (nm)	V_{total}[b] ($cm^3\ g^{-1}$)	V_p[c] ($cm^3\ g^{-1}$)	S_{BET}[d] ($m^2\ g^{-1}$)	d_{HK}[e] (nm)	d_{BdB}[f] (nm)	$T_{w\ BdB}$[g] (nm)	C
1Ti-MS-T-cal	4.3	1.07	0.62	987	2.8	3.3	1.0	74
(1-1)VTi-MS-T-cal	4.4	1.05	0.60	939	2.8	3.3	1.1	80
(2.5-1)VTi-MS-T-cal	4.4	1.13	0.58	893	2.8	3.3	1.1	84
(5-1)VTi-MS-T-cal	4.8	1.26	0.53	825	2.8	3.4	1.4	89
2.5Ti-MS-T-cal	4.4	1.23	0.58	961	2.8	3.3	1.1	68
(1-2.5)VTi-MS-T-cal	4.4	1.20	0.54	900	2.8	3.3	1.1	77
(2.5-2.5)VTi-MS-T-cal	4.5	1.28	0.53	879	2.8	3.3	1.2	81
(5-2.5)VTi-MS-T-cal	4.8	1.39	0.52	814	2.8	3.3	1.5	82
5Ti-MS-T-cal	4.3	1.37	0.54	952	2.7	3.2	1.1	62
(1-5)VTi-MS-T-cal	4.4	1.45	0.51	919	2.7	3.3	1.1	68
(2.5-5)VTi-MS-T-cal	4.4	1.38	0.50	890	2.8	3.3	1.1	71
(5-5)VTi-MS-T-cal	4.9	1.47	0.47	837	2.8	3.3	1.6	76
10Ti-MS-T-cal	4.3	1.31	0.47	939	2.6	3.1	1.2	51
(1-10)VTi-MS-T-cal	4.2	1.43	0.44	897	2.7	3.3	0.9	57
(2.5-10)VTi-MS-T-cal	4.4	1.41	0.45	867	2.7	3.3	1.1	62
(5-10)VTi-MS-T-cal	4.7	1.54	0.43	831	2.7	3.3	1.4	64

(a) Same as Table S1

Table S2(b). Porosity data of **VAl-MS-L-cal** derived from N_2 sorption isotherms.

Sample	a_0[a] (nm)	V_{total}[b] ($cm^3\ g^{-1}$)	V_p[c] ($cm^3\ g^{-1}$)	S_{BET}[d] ($m^2\ g^{-1}$)	d_{HK}[e] (nm)	d_{BdB}[f] (nm)	$T_{w\ BdB}$[g] (nm)	C
1Al-MS-L-cal	4.5	1.41	0.76	1108	3.2	3.6	0.9	57
(1-1)VAl-MS-L-cal	4.6	1.54	0.83	1082	3.3	3.7	0.9	68
(2.5-1)VAl-MS-L-cal	4.7	1.74	0.74	1044	3.3	3.7	1.0	79
(5-1)VAl-MS-L-cal	4.7	1.34	0.70	926	3.2	3.7	1.0	82
2.5Al-MS-L-cal	4.7	1.62	0.67	985	3.2	3.7	1.0	68
(1-2.5)VAl-MS-L-cal	4.6	1.67	0.66	975	3.2	3.7	0.9	80
(2.5-2.5)VAl-MS-L-cal	4.7	1.62	0.64	916	3.2	3.7	1.0	89
(5-2.5)VAl-MS-L-cal	4.8	1.26	0.62	852	3.2	3.6	1.2	90
5Al-MS-L-cal	4.9	1.57	0.56	827	3.2	3.7	1.2	84
(1-5)VAl-MS-L-cal	4.9	1.52	0.57	822	3.2	3.6	1.3	87
(2.5-5)VAl-MS-L-cal	4.8	1.45	0.53	776	3.2	3.6	1.2	92
(5-5)VAl-MS-L-cal	5.0	1.34	0.48	725	3.1	3.6	1.4	92
10Al-MS-L-cal	#	1.46	0.34	652	3.0	3.5	#	86
(1-10)VAl-MS-L-cal	#	1.51	0.34	690	3.0	3.5	#	78
(2.5-10)VAl-MS-L-cal	#	1.39	0.30	672	2.9	3.4	#	74
(5-10)VAl-MS-L-cal	#	0.77	0.23	640	#	#	#	64

Table S2 (c). Porosity data of **VZr-MS-L-cal** and **VCe-MS-L-cal**.

Sample	a_0[a] (nm)	V_{total}[b] ($cm^3\ g^{-1}$)	V_p[c] ($cm^3\ g^{-1}$)	S_{BET}[d] ($m^2\ g^{-1}$)	d_{HK}[e] (nm)	d_{BdB}[f] (nm)	$T_{w\ BdB}$[g] (nm)	C
2.5Zr-MS-L-cal	4.4	1.47	0.59	905	2.9	3.6	0.8	78
(1-2.5)VZr-MS-L-cal	4.5	1.26	0.62	907	3.2	3.7	0.8	80
(2.5-2.5)VZr-MS-L-cal	4.5	1.28	0.75	1009	3.2	3.7	0.8	79
(5-2.5)VZr-MS-L-cal	4.6	0.97	0.54	745	3.2	3.7	0.9	80
2.5Ce-MS-T-cal	4.3	1.08	0.58	870	2.8	3.5	0.8	91
(1-2.5)VCe-MS-T-cal	4.6	1.12	0.58	876	2.8	3.5	1.1	90
(2.5-2.5)VCe-MS-T-cal	4.5	1.19	0.54	838	2.8	3.5	1.0	94
(5-2.5)VCe-MS-T-cal	4.7	1.60	0.47	781	2.8	3.5	1.2	92

Table S3. ^{27}Al NMR analysis of as-prepared **Al-MS-L** and **VAl-MS-L** samples.

Sample	Al (tet)	Al (oct)	Al (penta)
1Al-MS-L	100	0	0
(1-1)VAl-MS-L	100	0	0
2.5Al-MS-L	100	0	0
(1-2.5)VAl-MS-L	100	0	0
5Al-MS-L	99.2	0.8	0
(1-5)VAl-MS-L	99.5	0.5	0
10Al-MS-L	97.7	2.3	0
(1-10)VAl-MS-L	99.4	0.6	0

Table S4. ^{29}Si quantitative NMR analysis of as-prepared samples with V and Ti/Al/Zr/Ce anchors.

Sample	Q^4	width	Q^3	width	Q^2	Width
MS-L	64	8.5	31	6.5	5	6.7
2.5V-MS-L	61	8.7	33	8.4	6	6.7
2.5Ti-MS-T	50	8.9	42	7.8	8	6.7
2.5Al-MS-L	48	9.6	43	8.2	9	6.7
2.5Zr-MS-L	45	8.4	47	8.4	8	6.7
2.5Ce-MS-T	53	9.2	40	7.5	7	6.7
(2.5-2.5)VTi-MS-T	50	8.7	43	8.4	7	6.7
(2.5-2.5)VAl-MS-L	54	9.8	39	8.5	7	6.7
(2.5-2.5)VZr-MS-L	51	9.0	40	9.0	9	6.7
(2.5-2.5)VCe-MS-T	52	8.6	41	8.3	7	6.7

Q^4 (-109 ppm, silicon coordinated with four oxygen atoms), Q^3 (-99 ppm, each silicon atom coordinated with three oxygen atoms and one hydroxy group), and Q^2 (-91 ppm, each silicon atom coordinated with two oxygen atoms and two hydroxy groups).[4]

Table S5a. E_g from Tauc plots of Fig.S10a.

Sample	Energy (eV)
1Ti-MS-T-cal	-
(1-1)VTi-MS-T-cal	3.77
(2.5-1)VTi-MS-T-cal	2.87
(5-1)VTi-MS-T-cal	2.57
2.5Ti-MS-T-cal	-
(1-2.5)VTi-MS-T-cal	3.71
(2.5-2.5)VTi-MS-T-cal	3.56
(5-2.5)VTi-MS-T-cal	2.85
5Ti-MS-T-cal	-
(1-5)VTi-MS-T-cal	3.79
(2.5-5)VTi-MS-T-cal	3.65
(5-5)VTi-MS-T-cal	3.36
10Ti-MS-T-cal	-
(1-10)VTi-MS-T-cal	3.84
(2.5-10)VTi-MS-T-cal	3.65
(5-10)VTi-MS-T-cal	3.42

Table S5b. E_g from Tauc plots of Fig.S10b.

Sample	Energy (eV)
1Al-MS-L-cal	-
(1-1)VAl-MS-L-cal	2.80
(2.5-1)VAl-MS-L-cal	2.52
(5-1)VAl-MS-L-cal	2.38
2.5Al-MS-L-cal	-
(1-2.5)VAl-MS-L-cal	3.24
(2.5-2.5)VAl-MS-L-cal	2.57
(5-2.5)VAl-MS-L-cal	2.46
5Al-MS-L-cal	-
(1-5)VAl-MS-L-cal	3.49
(2.5-5)VAl-MS-L-cal	2.69
(5-5)VAl-MS-L-cal	2.55
10Al-MS-L-cal	-
(1-10)VAl-MS-L-cal	2.84
(2.5-10)VAl-MS-L-cal	2.65
(5-10)VAl-MS-L-cal	2.56

Table S5c. E_g from Tauc plots of Fig.S10b and Fig 10d.

Sample	Energy (eV)
2.5Zr-MS-L-cal	-
(1-2.5)VZr-MS-L-cal	2.90
(2.5-2.5)VZr-MS-L-cal	2.65
(5-2.5)VZr-MS-L-cal	2.55
5Zr-MS-L-cal	-
(1-5)VZr-MS-L-cal	3.38
(2.5-5)VZr-MS-L-cal	2.74
(5-5)VZr-MS-L-cal	2.69
(5-2.5)VCe-MS-T-cal	2.56

Table S6a. High throughput screening of 1,2-diphenyl-2-methoxyethanol oxidation using Ti anchoring ions.

Catalysts	**Conversion (%)**	**Selectivity (%)**			
		Benzaldehyde	Methyl benzoate	Methanol	Benzoin methyl ether
1Ti-MS-T-cal	0	-	-	-	-
(1-1)VTi-MS-T-cal	<1	-	-	-	-
(2.5-1)VTi-MS-T-cal	42	77	11	0	12
(5-1)VTi-MS-T-cal	52	79	8	6	7
2.5Ti-MS-T-cal	0	-	-	-	-
(1-2.5)VTi-MS-T-cal	<1	-	-	-	-
(2.5-2.5)VTi-MS-T-cal	8	100	0	0	0
(5-2.5)VTi-MS-T-cal	50	81	6	6	7
5Ti-MS-T-cal	0	-	-	-	-
(1-5)VTi-MS-T-cal	<1	-	-	-	-
(2.5-5)VTi-MS-T-cal	<1	-	-	-	-
(5-5)VTi-MS-T-cal	31	90	0	0	10
10Ti-MS-T-cal	0	-	-	-	-
(1-10)VTi-MS-T-cal	<1	-	-	-	-
(2.5-10)VTi-MS-T-cal	<1	-	-	-	-
(5-10)VTi-MS-T-cal	7	100	0	0	0

Table S6b. High throughput screening of 1,2-diphenyl-2-methoxyethanol oxidation using Zr and Ce anchoring ions.

Catalysts	Conversion (%)	Selectivity (%)			
		Benzaldehyde	Methyl benzoate	Methanol	Benzoin methyl ether
2.5Zr_N-MS-L-cal	0	-	-	-	-
(1-2.5)VZr-MS-L-cal	<1	-	-	-	-
(2.5-2.5)VZr-MS-L-cal	29	100	-	-	0
(5-2.5)VZr-MS-L-cal	68	89	0	6	5
5Zr-MS-L-cal	0	-	-	-	-
(1-5)VZr-MS-L-cal	<1	-	-	-	-
(2.5-5)VZr-MS-L-cal	4	100	0	0	0
(5-5)VZr-MS-L-cal	39	94	0	0	6
2.5Ce-MS-T-cal	0	-	-	-	-
(1-2.5)VCe-MS-T-cal	4	100	0	0	0
(2.5-2.5)VCe-MS-T-cal	20	100	0	0	0
(5-2.5)VCe-MS-T-cal	50	87	6	7	0

Table S7. Oxidation of 1,2-diphenyl-2-methoxyethanol in different solvents via vanadium catalyst **(5-1)VAl-MS-L-cal**.

No.	Solvent	Boiling Point (ºC)	Polarity	Conversion (%)	Selectivity to Benzaldehyde (%)
1	Chloroform	61	4.4	93	65
2	Benzene	80	3.0	92	79
3	EtOAc	77	4.3	83	> 95
4	Toluene	111	2.4	70	> 95
5	MeCN	82	6.2	72	89
6	CH_2Cl_2	40	3.4	69	63
7	Dioxane	101	4.8	27	72
8	THF	66	4.2	23	57
9	DMSO	189	7.2	14	49
10	Pyridine	115	5.3	< 5	-
11	Ethanol (95 %)	78	4.3	< 5	-
12	H_2O (+MeCN)	100	10.2 (6.2)	< 5	-

Table S8. Recycling test of **(2.5-2.5)VAl-MS-L-cal** for 1,2-diphenyl-2-methoxyethanol oxidation in acetonitrile.

Catalysts	Conversion (%)	Selectivity (%)				
		Benzal-dehyde	Methyl benzoate	Methanol	Benzoic acid	Benzoin methyl ether
(2.5-2.5)VAl-MS-L-1st	49	84	10	6	0	0
(2.5-2.5)VAl-MS-L-2nd	46	81	12	4	0	3
(2.5-2.5)VAl-MS-L-3rd	43	79	13	5	0	3
(2.5-2.5)VAl-MS-L-4th	39	78	14	5	0	3
(2.5-2.5)VAl-MS-L-cal[a]	32	76	19	0	0	5

a) After leaching in MeOH.

References

[1] Chen, Y.; Yang, G.; Zhang, Z.; Yang, X.; Hou, W.; Zhu, J.-J. Polyaniline-intercalated layered vanadium oxide nanocomposites—One-pot hydrothermal synthesis and application in lithium battery. *Nanoscale* **2010**, *2*, 2131-2138.
[2] Sanchez, C.; Livage, J.; Lucazeau, G. Infrared and Raman study of amorphous V_2O_5. *J. Raman Spect.* **1982**, *12*, 68-72.
[3] Parambadath, S.; Mathew, A.; Park, S.S.; Ha, C.-S. Pentane-1, 2-dicarboxylic acid functionalized spherical MCM-41: A simple and highly selective heterogeneous ligand for the adsorption of Fe^{3+} from aqueous solutions. *J. Environ. Chem. Eng.* **2015**, *3*, 1918-1927.
[4] Chaignon, J.; Bouizi, Y.; Davin, L.; Calin, N.; Albela, B.; Bonneviot, L. Minute-made and low carbon fingerprint microwave synthesis of high quality templated mesoporous silica. *Green Chem.* **2015**, *17*, 3130-3140.